Catal Lett (2008) 126:346–352
DOI 10.1007/s10562-008-9629-8

A Highly Efficient Hβ Zeolite Supported Pt Catalyst Promoted by Chromium for the Hydroisomerization of *n*-Heptane

Ping Liu · Jun Wang · Ruiping Wei ·
Xiaoqian Ren · Xingguang Zhang

Received: 16 June 2008 / Accepted: 25 August 2008 / Published online: 19 September 2008

Abstract Hβ zeolite supported Pt catalysts promoted by Cr, La, Ce, Al or Zn were prepared by the co-impregnation method, and characterized by XRD, BET, NH_3-TPD and H_2-TPR. Their catalytic activities were evaluated in the hydroisomerization of *n*-heptane with an atmospheric fixed-bed reactor. The Pt-bearing catalyst doped with Cr, La or Ce, especially Cr, is found to exhibit a much higher catalytic activity and isomerization selectivity than the catalyst without the dopant. At the low reaction temperature of 230 °C, the catalyst with a Pt loading of 0.4% and a molar ratio of Cr to Pt of 5:1 shows a high conversion of *n*-heptane of 77.1% coupled with a high selectivity to isomerization products of 94.4%. In contrast, over the counterpart catalyst without Cr, the conversion of *n*-heptane is 50.6% with a low selectivity to isomerization products of 82.4%. The substantial promotion effect of Cr is suggested to associate with the improved Pt dispersion, as well as the increased strong acid amount, due to the introducing of Cr into the catalyst.

Keywords Hydroisomerization · *n*-Heptane · Beta zeolite · Bimetal catalyst

1 Introduction

In refineries, skeletal isomerization of light *n*-paraffins is an important environmentally friendly process to enhance the octane number in gasoline pool. Hydroisomerization of C_5/C_6 has been used as a commercial approach to light isoparaffins, where chlorinated Pt/Al_2O_3 or Pt/mordenite was used as the catalyst [1]. Nowadays, hydroisomerization of the paraffins from C_7 to C_9 is highly desirable to improve the isomerization selectivity with decreasing the cracking [2]. *n*-Heptane is usually used as a model reactant for the hydroisomerization of long chain paraffins. However, *n*-heptane would crack largely over the conventional Pt/mordenite catalyst [3]. So, many researchers have been seeking the effective catalysts for hydroisomerization of *n*-C_7 to promote the selectivity to branched paraffins [3–6], in which the bifunctional catalysts, such as Pt-Hβ zeolite [3], Pt–Y zeolite [4], Pt- or Pd-promoted heteropolyacids [5, 6] have attracted much attention.

Mordenite, ZSM-5, USY and β zeolites have been employed as acidic sites in bifunctional catalysts for the hydroisomerization of alkanes [7–10], and β zeolite has attracted a great industrial interest for its favorable acidity and pore system [11]. Chica et al. [3] revealed that the Pt-supported nanocrystalline β zeolite catalyst showed much higher selectivity for branched heptanes in *n*-heptane hydroisomerization than Pt/mordenite did. Leu et al. [12] observed a higher activity and isomerization selectivity over Pt/Hβ for *n*-hexane transformation than those over Pt/H-mordenite, Pt/HY and Pt/H-ZSM-5. They attributed this enhancement to the presence of large intersecting pores in β framework. López et al. [13] compared the activity and selectivity in the hydroconversion of *n*-pentane on Pt-containing HZSM-5, Hβ and SAPO-11 catalysts, and found that the Pt/HDβ (dealuminated Hβ) catalyst showed the best performance at the reaction temperature of 300 °C with high activity, stability and selectivity to isopentanes.

On the other hand, some reports introduced a second metal into the supported Pt catalysts to improve the catalytic activity, selectivity and stability for isomerization of

---

P. Liu · J. Wang (✉) · R. Wei · X. Ren · X. Zhang
State Key Laboratory of Materials-Oriented Chemical Engineering, College of Chemistry and Chemical Engineering, Nanjing University of Technology, Nanjing 210009, China
e-mail: junwang@njut.edu.cn

n-paraffins [14–17]. Fabio et al. [15] observed an increase in the selectivity for isomerization and aromatization products by doping In or Sn into Pt/Al_2O_3 catalysts. Mao et al. [16] found a significantly enhanced yield of branched paraffins by the incorporation of a small amount of Al^{3+} species into the HY zeolite together with the Pt species. Wei et al. [18, 19] recently studied the hydroisomerization of *n*-heptane over Pt catalysts supported on ultra-stable Y zeolite together with phosphotungstic acid or SO_4^{2-}/ZrO_2, and observed that these catalysts were substantially promoted by doping with Cr, Ce or La in catalytic activity, stability and selectivity for isomerization.

Based on the advantages of β zeolite as the acidic support and the bimetal system (a noble metal and a second metal), in this work, we study the hydroisomerization of *n*-heptane over the Hβ zeolite supported Pt catalysts doped with Cr, La, or Ce as the promoter, and find a highly improved catalytic conversion of *n*-heptane with a high isomerization selectivity for isoheptanes due to the promotion effect of the second metal.

2 Experimental

Hβ was prepared by the repeated ion-exchange of Naβ (Commercially delivered by Fushun No. 3 Petrochemical Factory, CNPC) with the aqueous solution of NH_4NO_3, followed by washing with deionized water, drying at 110 °C for 12 h and calcination at 550 °C for 3 h. The Hβ supported Pt catalysts doped with Cr, La, Ce, Al or Zn were designated as *m*M*n*Pt/Hβ, where M stands for Cr, La, Ce, Al or Zn, *m* stands for the molar ratio of M to Pt, *n* stands for the Pt loading by weight percentage. They were obtained by impregnation. In detail, Hβ zeolite was immersed in a mixed aqueous solution of chloroplatinic acid ($0.0058\ \mathrm{mol\ L^{-1}}$) and $Cr(NO_3)_3$ ($La(NO_3)_3$, $Ce(NO_3)_3$, $Al(NO_3)_3$ or $Zn(NO_3)_2$) ($0.0290\ \mathrm{mol\ L^{-1}}$) with the preset contents of Pt and Cr (La, Ce, Al or Zn) to meet the different composites of catalysts, followed by drying at 110 °C for 12 h and calcination at 400 °C for 3 h. The loading of Pt in catalysts was 0.05–1.0% by weight and the molar ratio of M to Pt was 0:1, 1:1, 5:1, 10:1 and 15:1, respectively.

Hydroisomerization of *n*-heptane was carried out in an atmospheric fixed-bed flow reactor. 0.565 g of the granular catalyst (40–60 mesh) was charged in the middle stage of the stainless steel tubular reactor. The catalyst was reduced in situ in H_2 flow at 300 °C for 3 h before reaction. Reaction conditions were as follows: 190–290 °C of reaction temperature, $2.7\ \mathrm{h^{-1}}$ of weight hourly space velocity, and 7.9 of molar ratio of H_2 to *n*-heptane. The product mixture was quantitatively analyzed online by the gas chromatograph (SHIMADZU GC-2014) equipped with a SE30 capillary column (50 m × 0.25 mm × 0.3 μm) and FID. The products were qualitatively confirmed by GC-MS (ThermoFinnigan).

The powder X-ray diffraction (XRD) patterns for catalysts were collected on a Bruker D8 ADVANCE X-ray diffractometer using Cu Kα radiation at 40 kV and 30 mA with a scan rate of $2\ \mathrm{min^{-1}}$, scanning range of 5–50°. BET surface areas were calculated by N_2 adsorption data from the Coulter Ommisorp 100CX equipment. Temperature-programmed desorption of ammonia (NH_3-TPD) and temperature-programmed reduction of hydrogen (H_2-TPR) were conducted using a JAPAN BELCAT-Analyzer. For NH_3-TPD, 200 mg of sample was placed into a quartz tube and pretreated at 500 °C for 2 h under a flow of helium. After the system was cooled to 100 °C, ammonia was introduced into the quartz tube. Later, the sample was purged with helium for 40 min in order to eliminate physisorbed species. Subsequently, the sample was heated from 100 to 550 °C at a heating rate of $10\ \mathrm{°C\ min^{-1}}$. For H_2-TPR, the loaded sample in quartz tube was pretreated at 400 °C for 1 h under a flow of oxygen followed with cooling to 50 °C and swept with argon for 20 min. While the sampled was heated at a mixture of hydrogen and argon at a heating rate of $10\ \mathrm{°C\ min^{-1}}$ up to 650 °C, the temperature and consumption of hydrogen were respectively recorded.

3 Results and discussion

XRD patterns of Hβ, 0.4%Pt/Hβ and various 5M0.4%Pt/Hβ catalysts are illustrated in Fig. 1. It shows that the XRD curves of all metal-bearing catalysts are more or less very similar to that of pure Hβ zeolite. The support well keeps the pore structure of β zeolite. No diffraction peaks assigned to Cr, La, Ce, Al or Zn oxide occur for all 5M0.4%Pt/Hβ catalysts. For 0.4%Pt/Hβ, The peak at 2θ of 39.8° assigned to Pt (111) can be detected, although it is not in a clear sharp shape. However, for 5Al0.4%Pt/Hβ and 5Zn0.4%Pt/Hβ, the Pt (111) peaks can be clearly observed, indicating that the additive Al or Zn leads to a lowed dispersion of Pt on support. While for the other catalysts (5Ce0.4%Pt/Hβ, 5Cr0.4%Pt/Hβ, and 5La0.4%Pt/Hβ), the peak for Pt (111) can not be detected. This demonstrates that the addition of Cr, La or Ce into the Pt/Hβ catalyst can evidently increase the dispersion of Pt on the surface of Hβ support.

Figure 2 gives the XRD patterns for the catalysts with different Pt loadings. It can be seen that all the XRD patterns of the catalysts are exactly same as the Hβ support even at a high Pt loading of 1.0% without observing any diffraction peaks for Pt. A similar phenomenon is observed for the catalysts with the molar ratio of Cr to Pt from 1:1 to

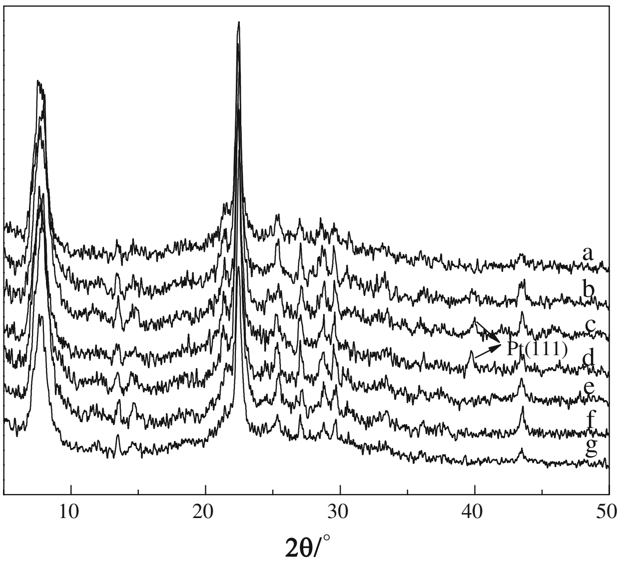

Fig. 1 XRD patterns of Hβ, 0.4%Pt/Hβ and various 5M0.4%Pt/Hβ catalysts (a) Hβ, (b) 0.4%Pt/Hβ, (c) 5Al0.4%Pt/Hβ, (d) 5Zn0.4%Pt/Hβ, (e) 5Ce0.4%Pt/Hβ, (f) 5Cr0.4%Pt/Hβ, (g) 5La0.4%Pt/Hβ

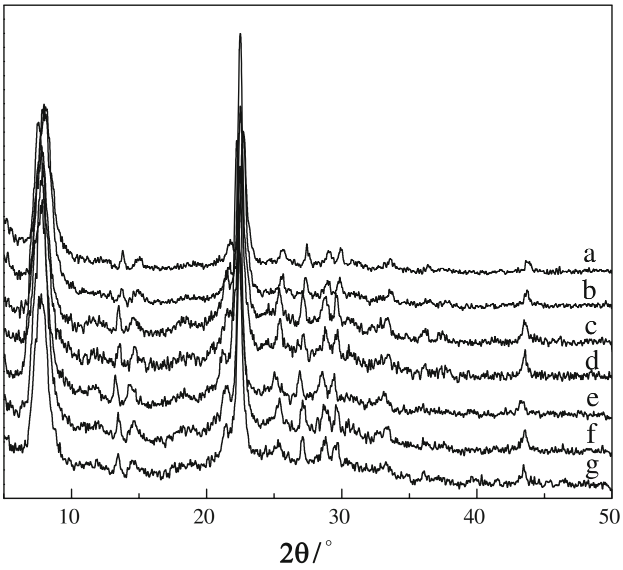

Fig. 2 XRD patterns of catalysts with different Pt loadings (a) Cr0.05%Pt/Hβ, (b) Cr0.1%Pt/Hβ, (c) Cr0.2%Pt/Hβ, (d) Cr0.4%Pt/Hβ, (e) Cr0.6%Pt/Hβ, (f) Cr0.8%Pt/Hβ, (g) Cr1.0%Pt/Hβ

15:1 (XRD patterns not shown). This tells that the crystal sizes of Pt metal and Cr oxides on the support are not large enough to be detected by XRD, which means the high dispersion of Pt on the surface of Hβ due to the addition of Cr into catalysts.

Table 1 lists the BET surface areas of various catalysts. It can be seen that the Hβ support exhibits a high surface area of 575 $m^2 g^{-1}$. When Pt and a second metal were supported onto the Hβ, the surface areas of catalysts only slightly decrease with a relatively high value around 530 $m^2 g^{-1}$. Meanwhile, the surface area of 10Cr0.4%Pt/Hβ further drops to 480 $m^2 g^{-1}$ with a very high molar ratio of Cr to Pt of 15:1.

Table 1 BET surface areas of various Hβ supported catalysts

Catalyst	S_{BET}/($m^2 g^{-1}$)	Catalyst	S_{BET}/($m^2 g^{-1}$)
Hβ	575	5La0.4%Pt/Hβ	522
0.4%Pt/Hβ	529	5Cr0.4%Pt/Hβ	514
5Al0.4%Pt/Hβ	538	10Cr0.4%Pt/Hβ	506
5Zn0.4%Pt/Hβ	546	15Cr0.4%Pt/Hβ	480
5Ce0.4%Pt/Hβ	534		

Temperature-programmed desorption of ammonia profiles for various 5M0.4%Pt/Hβ catalysts are shown in Fig. 3. In all cases, the curves give two peaks at around 220 and 400 °C, corresponding to the desorption of ammonia on weak and strong acid sites, respectively. The peak positions almost do not shift upon the doping with those metals. Compared to 0.4%Pt/Hβ, 5Al0.4%Pt/Hβ and 5Zn0.4%Pt/Hβ possess slightly lowered amount of strong acid sites, and in contrast, the Cr- (Ce- or La-) doped sample shows a slightly increase in acid amount. In addition, the variation of Cr loading in *m*Cr0.4%Pt/Hβ catalysts

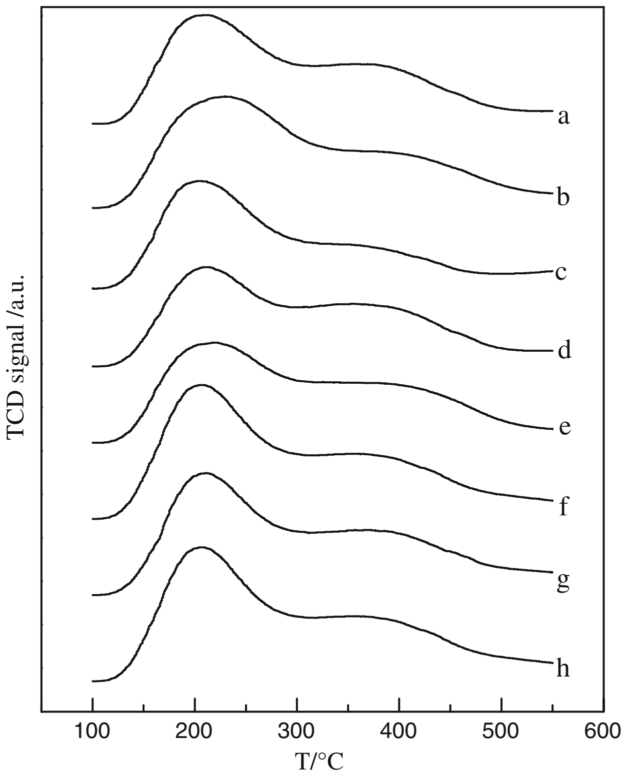

Fig. 3 NH_3-TPD profiles of various *m*M0.4%Pt/Hβ catalysts (a) 0.4%Pt/Hβ, (b) 5Al0.4%Pt/Hβ, (c) 5Zn0.4%Pt/Hβ, (d) 5Ce0.4%Pt/Hβ, (e) 5La0.4%Pt/Hβ, (f) 5Cr0.4%Pt/Hβ, (g) 10Cr0.4%Pt/Hβ, (h) 15Cr0.4%Pt/Hβ

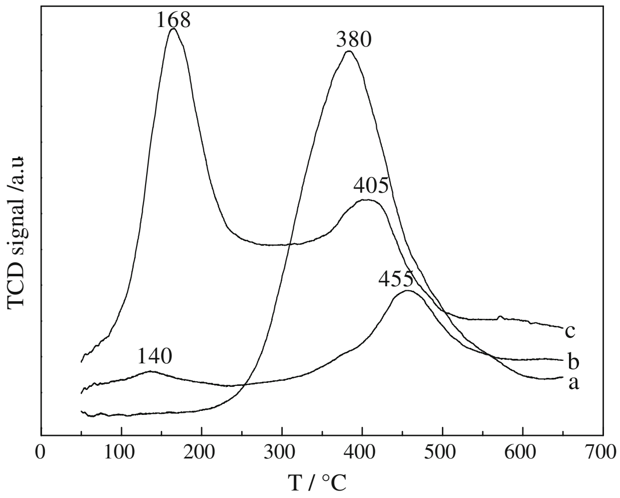

Fig. 4 H_2-TPR profiles of Cr/Hβ (a), 0.4%Pt/Hβ (b), and 5Cr0.4%Pt/Hβ (c)

exerts no clear impact on the catalyst acidity, also as shown in Fig. 3.

Figure 4 compares H_2-TPR profiles of Cr/Hβ, 0.4%Pt/Hβ and 5Cr0.4%Pt/Hβ. Cr/Hβ sample with the Cr loading being equal to that for 5Cr0.4%Pt/Hβ presents a large hydrogen consumption peak at 380 °C, which can be associated with the reduction of Cr_2O_3 species according to the previous literature [20]. 0.4%Pt/Hβ catalyst gives a small peak at a low temperature of 140 °C and a moderate one at around 455 °C. The former small peak is for the reduction of PtO_2 and PtO located in zeolite channels [21], while the latter one indicates the strong interaction of Pt^{2+} with β zeolite with the formation of $\mathrm{Pt}-(\mathrm{O}-\mathrm{Si}\equiv)_y^{2-y}$ species [22, 23]. The bimetallic catalyst 5Cr0.4%Pt/Hβ exhibits two reduction peaks: a large peak at around 168 °C and a comparatively small peak at around 405 °C. It is clear that the curve for 5Cr0.4%Pt/Hβ is not a result of the simple overlapping of the profiles of the two monometallic samples, which implies a strong interaction of Cr and Pt. Furthermore, it suggests that much larger proportion of Pt species in 5Cr0.4%Pt/Hβ can be reduced at a low temperature of 168 °C. This may be favorable to the hydrogenation–dehydrogenation function at metal sites for a bifunctional catalyst.

Table 2 shows the conversion of *n*-heptane, the selectivity to isomerized products and the yield of mono- and multi-branched isoheptanes over 0.4%Pt/Hβ and 5M0.4%Pt/Hβ catalysts at a reaction temperature of 230 °C and a reaction time on stream of 60 min. In this work, a stabilized conversion and selectivity can be obtained after 60 min on stream over all catalysts. It is seen that a considerable conversion of *n*-heptane of 50.6% with a low selectivity to isomerization of 82.4% is obtained over 0.4%Pt/Hβ. With the introducing of Al or Zn into the catalyst, the conversion drastically drops to a very low level along with a further decrease of the selectivity to isomerization. This may be understandable by the observation in Fig. 1 that the dispersion of Pt is lowed by the introducing of Al or Zn. On the other hand, the strong acid sites were revealed to be responsible to the isomerization reaction [24–26], therefore, another possible explanation for the decreased activity is ascribed to the decrease of the strong acid amount upon doping of Al or Zn, as shown in Fig. 3. What is notable in Table 2 is the simultaneously and remarkably increase of conversion of *n*-heptane, the selectivity to isomerized products and the yield of mono- and multi-branched isoheptanes with the introduction of Cr, La or Ce. Moreover, 5Cr0.4%Pt/Hβ exhibits a much high conversion of *n*-heptane of 77.1% combined with a high isomerization selectivity of 94.4%. This result is suggested to be relative to the improved Pt dispersion (see Fig. 1), the enhanced reducibility of Pt (see Fig. 4), as well as the increased strong acid amount (see Fig. 3), by introducing Cr, La or Ce.

Figure 5 displays the influence of Cr loading in *m*Cr0.4%Pt/Hβ ($m = 0$–15) catalysts on the catalytic activity and selectivity at 230 °C and 60 min on stream. It is found in Fig. 5 that all the Cr-doped catalysts show the higher catalytic activity and selectivity than 0.4%Pt/Hβ

Table 2 Catalytic activities of 0.4%Pt/Hβ and 5M0.4%Pt/Hβ catalysts for the hydroisomerization of *n*-heptane

Catalyst	Conversion (%)	Multi-branched products yield[a] (%)	Mono-branched products yield[b] (%)	Isomerization selectivity (%)
0.4%Pt/Hβ	50.6	8.0	33.7	82.4
5Al0.4%Pt/Hβ	12.9	1.3	8.1	72.9
5Zn0.4%Pt/Hβ	25.4	2.5	14.5	66.5
5Ce0.4%Pt/Hβ	56.7	10.7	43.8	96.0
5La0.4%Pt/Hβ	59.5	9.6	47.3	95.7
5Cr0.4%Pt/Hβ	77.1	18.0	54.8	94.4

[a] Multi-branched products include 2,2-dimethylpentane, 2,3-dimethylpentane, 2,4-dimethylpentane, 3,3-dimethylpentane and 2,2,3-trimethylbutane

[b] Mono-branched products include 2-methylhexane, 3-methylhexane and 3-ethylpentane

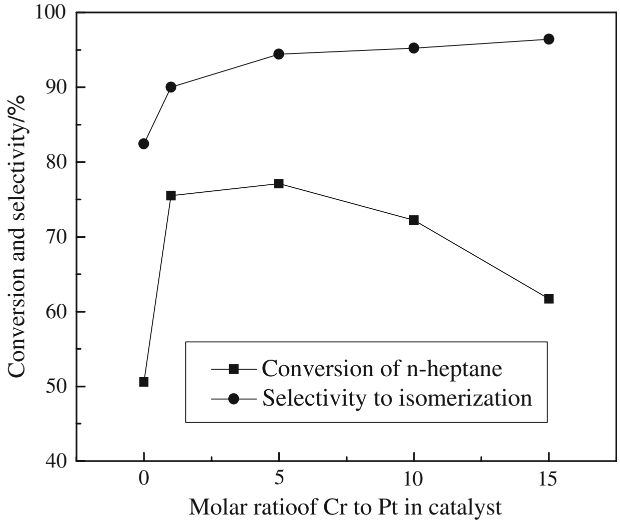

Fig. 5 Conversion of *n*-heptane and isomerization selectivity over the *m*Cr0.4%Pt/Hβ catalysts with different Cr loadings

does, which is true even at a low Cr content (Cr/Pt molar ratio of 1). The conversion of *n*-heptane decreases slowly with the increase of *m* from 5 to 15, and meanwhile the selectivity to isomerized products increases gradually all the way with the increase of *m*. Because the influence of the Cr loading on the dispersion of Pt and the acidity of catalyst is negligible (see Figs. 1 and 3), the decrease of conversion at high Cr loading maybe associates with the decrease of surface area due to the introduction of too much Cr species, which could hinder the access of reactant to the acid sites [27]. The above results suggest a suitable molar ratio of Cr/Pt of 5 for the catalyst *m*Cr0.4%Pt/Hβ.

Figure 6 shows the catalytic activity and selectivity as a function of Pt loading in CrnPt/Hβ catalysts, which possess a fixed Cr loading (the weight percentage of Cr_2O_3 is 1.6%) at 230 °C. It can be seen that the conversion of *n*-heptane increases very quickly with the increase of Pt content at low Pt loadings, and it reaches at a plateau value of around 75% when the Pt loading is up to 0.4%. Similarly, when the Pt loading exceeds 0.2%, the isomerization selectivity finds its constant value of around 95%. The optimal Pt loading of 0.4% can be proposed from Fig. 6. This observation is in agreement with the expectation of the classical bifunctional reaction mechanism for the hydroisomerization of paraffins, which tells that the acid and metal functions should match well with each other, and for a given acid support, there exists an optimal Pt loading to get a high activity and selectivity [28–30].

Figure 7 presents the conversion of *n*-heptane, the selectivities to various products and the yields of mono- and multi-branched isoheptanes at 230 °C over 5Cr0.4%Pt/Hβ catalyst as a function of WHSV. The conversion of *n*-heptane, multi-branched products yield and cracking selectivity all decrease with the increase of WHSV, while the isomerization selectivity increases. The mono-branched products yield is promoted with the increase of WHSV at low WHSV values and decreases at high WHSV. The cyclization selectivity keeps at a very low level when WHSV is altered from 1.4 to 5.5 h^{-1}. From Fig. 7, one can draw that the WHSV of 2.7 h^{-1} is the preferred selection for a well catalytic performance of the 5Cr0.4%Pt/Hβ catalyst.

Table 3 compares the catalytic activity of 5Cr0.4%Pt/Hβ with that of 0.4%Pt/Hβ at different reaction temperatures. For both catalysts, with the increase of reaction temperature, the conversion of *n*-heptane rises quickly accompanying with a quick decrease in the selectivity to isomerization. The exception occurs at a very low

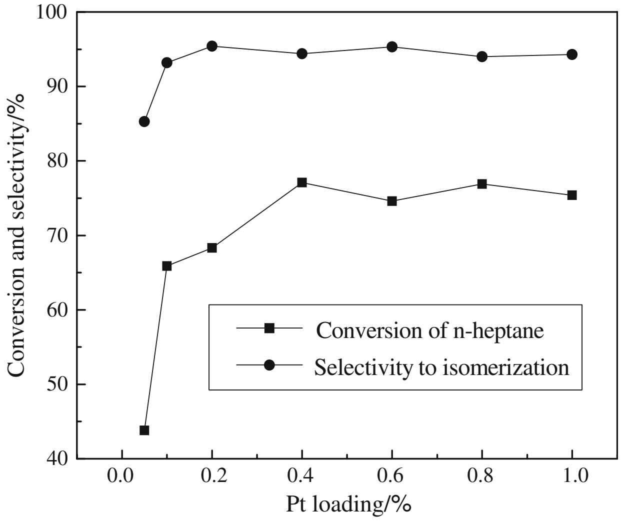

Fig. 6 Conversion of *n*-heptane and isomerization selectivity over the CrnPt/Hβ catalysts with different Pt loadings

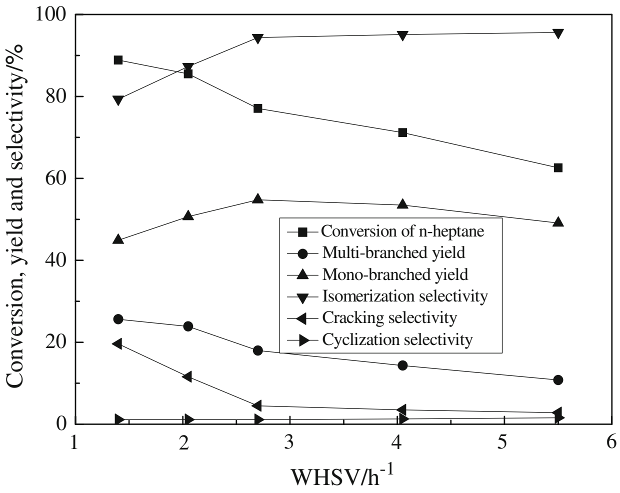

Fig. 7 Influence of WHSV on the catalytic performance of 5Cr0.4%Pt/Hβ in the hydroisomerization of *n*-heptane

Table 3 Comparison of the reactivity of hydroisomerization of *n*-heptane over the 0.4%Pt/Hβ and 5Cr0.4%Pt/Hβ catalysts at different reaction temperatures

Catalyst	*T* (°C)	Conversion (%)	Multi-branched products yield (%)	Mono-branched products yield (%)	Isomerization Selectivity (%)	Cyclization selectivity (%)
0.4%Pt/Hβ	190	9.4	0.6	7.0	81.1	18.2
	210	23.9	2.9	18.8	90.5	5.9
	230	50.6	8.0	33.7	82.4	1.9
	250	83.9	9.7	30.0	47.3	1.1
	270	97.3	5.0	10.7	16.1	1.1
	290	99.9	1.3	0.9	2.1	1.4
5Cr0.4%Pt/Hβ	190	9.4	0.2	7.8	84.3	14.3
	210	34.3	3.1	30.0	96.3	3.1
	230	77.1	18.0	54.8	94.4	1.1
	250	91.7	19.6	33.6	58.0	1.1
	270	96.7	8.7	13.4	23.0	1.1
	290	99.5	1.8	2.4	4.3	1.5

temperature of 190 °C, where the selectivity to isoheptanes is low duo to the selective generation of a large amount of cyclization products. A high isomerization selectivity of 94.4%, a high yield of isomerization products of 72.8%, and a high *n*-heptane conversion of 77.1% are obtained at 230 °C, which is proposed to be the optimal reaction temperature. In this case, the yield of multi-branched products amounts to a high value of 18.0%, which is very helpful for improving the octane number of gasoline pool. Moreover, at any of the reaction temperatures, both the conversion of *n*-heptane and the selectivity to isomerization over 5Cr0.4%Pt/Hβ are remarkably higher than those over 0.4%Pt/Hβ.

When the catalytic activity of 5Cr0.4%Pt/Hβ is compared with the Ce doped Pt-PW/DUSY (PW: phosphotungstic acid; DUSY: dealuminated ultra-stable Y zeolite) catalyst reported by Wei et al. [19] at the same reaction temperature of 230 °C, one can see that the two catalysts give very similar selectivity to isomerization products (94.4% vs. 95.8%), but the former shows a far higher *n*-heptane conversion than the later does (77.1% vs. 29.3%). Matsuda et al. [31] observed a high isomerization selectivity of 93.6% with *n*-heptane conversion of 51.4% at a reaction temperature of 250 °C; it is still obvious that the 5Cr0.4%Pt/Hβ catalyst in this work exhibits a higher conversion of 77.1% with a similar selectivity to isomerizatin of 94.4% even at a lower reaction temperature of 230 °C. These results further convince that 5Cr0.4%Pt/Hβ is a highly efficient catalyst for the hydroisomerization of *n*-heptane.

4 Conclusions

In the hydroisomerization of *n*-heptane, the Hβ zeolite supported Pt catalysts promoted by Cr, La or Ce are revealed to exhibit much higher catalytic activity and selectivity to isomerized products than the counterpart catalyst containing only Pt. And the catalyst doped with Cr shows the highest catalytic activity. Over the 5Cr0.4%Pt/Hβ catalyst at a reaction temperature of 230 °C, the conversion of *n*-heptane reaches 77.1% with a high selectivity to isomerization products of 94.4%. The high activity and selectivity of the 5Cr0.4%Pt/Hβ catalyst is suggested to associate with the improved Pt dispersion, as well as the increased strong acid amount, due to the introducing of Cr into the catalyst.

Acknowledgments The authors thank the Natural Science Foundation of China (No. 20476046) and the "Qinglan" Project of Jiangsu Province for Young Researchers.

References

1. Tromp M, van Bokhoven JA, Garriga Oostenbrink MT, Bitter JH, de Jong KP, Koningsberger DC (2000) J Catal 190:209
2. Marcilly C (2001) Stud Surf Sci Catal 135:37
3. Chica A, Corma A (1999) J Catal 187:167
4. Patrigeon A, Benazzi E, Travers C, Bernhard JY (2001) Catal Today 65:149
5. Atsuyuki M, Ryuichiro O, Toshio O (2004) Appl Catal A Gen 262:143
6. Wang J, Jiang DM, Baeg JO, Lee CW (2004) J Ind Eng Chem 10:454
7. Chao KJ, Leu CL (1996) Appl Catal A Gen 143:223
8. Brito A, García FJ, Alvarez-Galván MC, Borges ME, Díaz C, de la Peña O'Shea VA (2007) Catal Commun 8:2081
9. Pope TD, Kriz JF, Stanciulescu M, Jacques M (2002) Appl Catal A Gen 233:45
10. Wang ZB, Kamo A, Yoneda T (1997) Appl Catal A Gen 159:119
11. Treacy MMJ, Newsam JM (1988) Nature 332:249
12. Leu IJ, Hou LY, Kang BC, Li CP, Wu ST, Wu JC (1991) Appl Catal 69:49
13. López CM, Guillén Y, García L, Gómez L, Ramírez Á (2008) Catal Lett 122:267

14. Blomsma E, Martens JA, Jacobs PA (1997) J Catal 165:241
15. Fabio BP, Donato A, Aranda G (1998) J Catal 178:478
16. van Mao RL, Saberi MA (2000) Appl Catal A Gen 199:99
17. Martins A, Silva JM, Ribeiro FR (2006) Catal Lett 109:83
18. Wei RP, Wang J, Gu YB (2007) React Kinet Catal Lett 90:315
19. Wei RP, Gu YB, Wang J (2008) Sci China Ser B Chem 51:120
20. Araujo LRR, Schmal M (2002) Appl Catal A Gen 235:139
21. Jiménez C, Romero FJ, Gómez JP (2001) Recent Res Dev Pure Appl Chem 5:1
22. Zheng J, Dongand JL, Xu QH (1994) Stud Surf Sci Catal 84:1641
23. Roldán R, Beale AM, Sánchez-Sánchez M, Romero-Salguero FJ, Jiménez-Sanchidrián C, Gómez JP, Sankar G (2008) J Catal 254:12
24. Kinger G, Vinek H (2001) Appl Catal A Gen 218:139
25. Park K, Ihm S (2000) Appl Catal A Gen 203:201
26. Zhang W, Smirniotis PG (1999) J Catal 182:400
27. Fúnez A, de Lucas A, Sánchez P, Ramos MJ, Valverde JL (2008) Chem Eng J 136:267
28. Thybaut JW, Narasimhan CSL, Denayer JF, Baron GV, Jacobs PA, Martens JA, Marin GB (2005) Ind Eng Chem Res 44:5159
29. Yoshioka CMN, Garetto T, Cardoso D (2005) Catal Today 107–108:693
30. Wang J, Li QZ, Yao JD (1999) Appl Catal A Gen 184:181
31. Matsuda T, Watanabe K, Sakagami H, Takahashi N (2003) Appl Catal A Gen 242:267